Ranking Diffusion MRI Models for Fibre Dispersion using In Vivo Human Brain Data

Uran Ferizi[1,2], Torben Schneider[2], Eleftheria Panagiotaki[1], Maira Tariq[1], Hui Zhang[1], Claudia A. M. Wheeler-Kingshott[2], and Daniel C. Alexander[1]

[1]*Department of Computer Science and Centre for Medical Image Computing, University College London, London, United Kingdom,* [2]*NMR Research Unit, Department of Neuroinflammation, Queen Square MS Centre, UCL Institute of Neurology, London, United Kingdom*

Target Audience: Clinicians/physicists interested in brain microstructure imaging.

Purpose: To compare parametric diffusion MRI models, which explicitly seek to capture fiber dispersion, using *in-vivo* human brain data.

Introduction: Diffusion MRI probes the tissue microstructure by measuring water dispersion in biological tissue. Currently, the standard model for imaging diffusion in tissue is the diffusion tensor (DT), which is adequate only for describing major tissue damage. A recent class of parametric models has emerged to describe data better, and provide more sensitivity and the specificity, by additionally accounting for fiber directional incoherence, which is abundant in the brain, even at a sub-voxel level.

Methods: **Data acquisition and pre-processing:** We use a PGSE EPI sequence on a 3T Phillips scanner, with cardiac gating and TR=4s. The full protocol uses 32 HARDI shells. Each shell has a unique set of 45 directions. The protocol has a wide range of b-values, 218 to 10,308 s/mm^2, combining $\delta = \{6, 10, 15, 22\}$ms, $\Delta = \{30, 50, 70, 90\}$ms, $|\mathbf{G}| = \{55, 60\}$mT/m, and three interwoven b=0 s/mm^2 acquisitions. The data is acquired from a healthy male's corpus callosum (CC), in two separate non-stop sessions, each lasting 4.5h. We fit the DT to b=1,202 shell to select a set of voxels with coherently oriented principal directions. Voxels with FA>0.6 and principal eigenvector within 2◦ of the assumed fiber direction are retained and averaged. Fig. 1 shows this signal. **Model Construction:** *Extracellular Compartments:* Tensor (modelled through the DT), Zeppelin (cylindrically symmetric Tensor), Zeppelin with tortuosity (as in [1]) and Ball (isotropic Tensor). *Intracellular Compartments:* Sticks are used to represent the axonal diffusion, via either a discrete set of two Sticks [2] or an underlying Bingham/Watson fiber orientation distribution [3,4,5]. The Bingham distribution is similar to a bivariate Gaussian distribution with elliptical contours on the sphere; the Watson is a special case of Bingham, tracing circular contours on the sphere. **Model Fitting and Selection:** We use the *Camino* toolkit to fit the models. Each model is fitted 250 times, using the Levenberg-Marquardt algorithm with a perturbed starting point from initial estimates drawn from the DT, to extract the best parameters.

Results: **Table 1** shows the ranking, where single mode orientation distributions (Watson or Bingham) outperform two discrete orientations (two-Sticks), and where four groups can be distinguished:
i) combinations that include an anisotropic extracellular compartment with Bingham/Watson (in red);
ii) models similar to (i) but using two-Sticks for their intracellular compartment, excluding models that use tortuosity or those without a spherically restricted compartment (in blue);
iii) models incorporating an isotropic extracellular compartment with a Bingham or Watson (in green);
iv) all exceptions to two-Sticks models in (ii) (in grey).
As in previous work on this topic [6, 7], an anisotropic extracellular compartment benefits the fitting, as does the addition of an isotropically restricted compartment. **Fig.2** shows the fit of some models, to illustrate the difference between raw signal and that generated from models' best parameter estimates. Bootstrap and cross-correlation analysis (not shown) indicates that the division of the models into the four groups above is consistent across randomization, but the ranking of the models can permute within the groups.

Discussion: In CC, where various fiber tracts bundle together, there is inhomogeneity that can produce a dispersion pattern, which these models may reflect. Averaging voxels across the CC and minor misalignments during registration may exaggerate the dispersion; future work will study smaller ROIs. We also intend to extend the investigation to other white matter structures that have greater dispersion. The findings help identify the best models for future microstructure imaging of the brain with diffusion MRI. Experiment design optimization [8] will enable us to find economical protocols to support estimation of those models' parameters in practical imaging applications.

Conclusions: Models that capture fiber dispersion (Watson/Bingham) explain diffusion MRI data from in-vivo human white matter better than undispersed models (one or two sticks) even in apparently coherent fibers.

References: **[1]** Szafer A, et al.: Theoretical model for water diffusion in tissues. MRM 1995; **[2]** Behrens TE, et al.: Characterization and propagation of uncertainty in DW MR imaging. MRM, 2003; **[3]** Mardia KV, Jupp PE: Distributions on spheres. Dir.Stats., 2000; **[4]** Zhang H, et al.: Practical in vivo neurite orientation dispersion and density imaging of the human brain. NIMG 2012; **[5]** Sotiropoulos S, et al.: Inferring Fiber Fanning from Diffusion-weighted MRI. NIMG 2012; **[6]**: Panagiotaki E, et al. Compartment models of the diffusion MR signal in brain white matter: A taxonomy and comparison, NIMG, 2012; **[7]**: Ferizi U, et al.: Using in-vivo human brain data to select diffusion MRI compartment models, ISMRM, 2013. ; **[8]**: Alexander DC, A general framework for experiment design in diffusion MRI and its application in measuring direct tissue-microstructure features, MRM, 2008

Acknowledgements: EPSRC support this work through grants EP/E007748 and EP/I027084/01. The MS Society of Great Britain and NI, and NIHR/UCL-UCLH BRC, support the NMR unit.

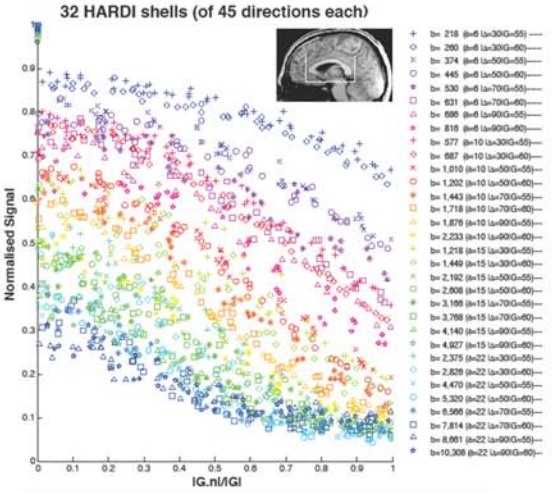

Fig.1: Signal data. The legend gives b-value (δ | Δ | $|G|$).

LSE	S0	Nr Parameters	MODELS	Vol. Fraction	Diffusivity (10^{-3} m^2/s)	Theta/ arc degree°	Phi/ arc degree°	Psi/ arc degree°	Vol. Fraction	Rad. Diff 1 (10^{-3} m^2/s)	Rad. Diff 2 (10^{-3} m^2/s)	Alpha/ arc degree°	Vol. Fraction	Theta/ arc degree°	Phi/ arc degree°	CSF/Dot Vol. Fract.
				Stick1/Watson/Bing					Ball/Zep/Ten.				Stick2			
481	1.00	10	Zepp.Bing.CSF.	0.56	2.0	74	89	1	0.29	0.5						0.15
511	1.00	7	ZepT.Wat.CSF.	0.59	2.0	89	1		0.28	0.6						0.13
512	0.98	10	Zepp.Bing.Dot	0.50	2.1	71	89	1	0.45	0.9						0.04
526	0.98	11	Tens.Bing.	0.65	2.2	67	89	1	0.35	1.2	0.9	55				
550	0.98	8	ZepT.Bing.	0.62	2.2	74	89	1	0.38	0.8						
614	0.97	12	Tens.St.St.Dot	0.23	2.0	86	4		0.56	0.8	0.7	20	0.14	75	14	0.07
635	1.00	12	Tens.St.St.CSF.	0.22	1.5	86	5		0.41	0.5	0.3	25	0.17	74	18	0.21
703	1.01	8	Ball.Bing.	0.72	2.2	75	88	1	0.28							
703	1.01	9	Ball.Bing.CSF.	0.72	2.2	74	89	1	0.28							0.00
761	**0.96**	**7**	**Zepp.St.Dot**	**0.29**	**1.9**	**89**	**1**		**0.62**	**0.7**						**0.09**
801	**1.00**	**10**	**Tens.Cylinder+CSF.**	**0.29**	**1.3**	**89**	**1**		**0.47**	**0.3**	**0.3**	**12**				**0.24**
814	0.98	9	ZepT.St.St.Dot	0.33	1.8	86	2		0.50	1.1			0.12	69	12	0.05
824	0.96	11	Tens.St.St.	0.28	1.7	84	5		0.52	0.9	0.7	29	0.20	70	17	
852	0.99	9	ZepT.St.St.CSF.	0.35	1.5	86	2		0.39	0.9			0.13	66	13	0.12
870	0.97	8	ZepT.St.St.	0.32	1.6	84	4		0.50	1.0			0.18	71	13	
1135	0.99	8	Ball.St.St.	0.28	1.5	80	6		0.46				0.25	75	10	

Table.1: Ranking for some representative models, as well as various model parameters. We also include the estimates (shown in bold) from the best model of a previous ranking of non-dispersive parametric models [7].

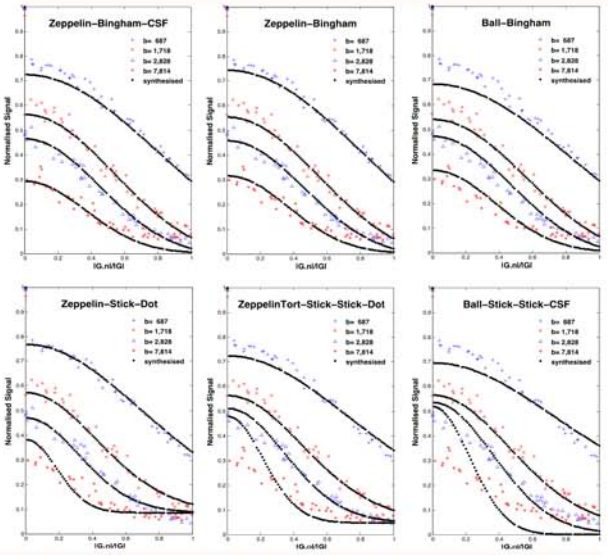

Fig.2: Comparing raw with synthesized signal in six representative models. The models are ordered in decreasing ranking left-right, top-bottom.